

# Intermetallic studies on the mechanical and dynamical properties of $\text{Fe}_{1-x}\text{Y}_x\text{Al}$ ( $\text{Y} = \text{Pt}$ and $\text{Ru}$ ) Alloys

Chrestinah S. Mkhonto<sup>1\*</sup>, Ndanduleni L. Lethole<sup>2</sup>, Phuti E. Ngoepe<sup>1</sup> and Hasani R. Chauke<sup>1</sup>

<sup>1</sup>Materials Modelling Centre, School of Physical and Mineral Sciences, Department of Physics, University of Limpopo, Private bag X1106, Sovenga 0727, South Africa.

<sup>2</sup>Department of Physics, University of Fort Hare, Alice 5700, South Africa; nlehole@ufh.ac.za.

**Abstract.** First-principles calculations were performed to determine the effect of Pt and Ru ternary alloying on structural, mechanical and dynamical properties of the binary Pm-3m-FeAl. FeAl based alloys are important for high-temperature applications due to their high oxygen corrosion resistance. Moreover, they are a major driver as a component for better infrastructure, industrial coating, and the improvement of automotive parts. The density functional theory (DFT) method within the generalized gradient approximation (GGA) approach was employed to perform all the calculations. The equilibrium cell parameters of the binary FeAl were predicted to be more than 90% in good agreement with the experimental data, warranting the validity of the approach employed. We found that Pt and Ru ternary alloying on FeAl significantly enhances the mechanical hardness, ductility and dynamical stability.

**Keywords:** Stability, ductility, hardness, phonon dispersion curve.

## 1. Introduction

Iron-aluminides (Fe-Al) alloys have attracted attention in various industrial sectors due to their superior resistance to oxygen corrosion and oxidation at high temperatures which exceed those of Ni-based superalloys [1]. The strong resistance to oxygen corrosion is due to a well-adherent protective oxide layer that forms on the surface of the metal interface. Fe-Al alloys have particularly attracted attention in the automotive sector where Advanced High Strength Steel (AHSS) improvement is necessary for the development of lightweight steel grades, leading to improved vehicle performance, reduced vehicle weight, fuel efficiency, and cost reduction [2].

Furthermore, the extraordinary resistance to oxidation at high temperatures makes these alloys to be potential candidates for steel substitutes and in water pipes for steel-coating. However, these alloys have been reported to suffer a sharp drop in strength at room temperature making them less significant for use as structural materials [3]. They are susceptible to fractures and ductility degradation at low temperatures hence suitable for high-temperature applications. The fractures are mainly induced by cracks on the surface as a result of low free surface energies [4]. They are known to be easily influenced by environmental conditions such as humidity and creep. Doping with platinum group metals (PGM's) and

---

\* Corresponding author: [chresimkhonto@gmail.com](mailto:chresimkhonto@gmail.com)

ruthenium have been widely reported to have a positive effect on the corrosion resistance of stainless steel such as titanium alloys. It is reported that doping led to the development of new grades to extend the operating window for titanium alloys [5, 6]. Hence, ternary alloying by platinum and ruthenium is considered in this study to enhance the corrosion properties and strength of Fe-Al alloy at ambient conditions. These two metals (platinum and ruthenium) are most suitable for strength enhancement due to their excellent ductility and high melting point [1, 7].

Under oxidizing conditions, aluminide coatings offer a protective oxide scale. By selective oxidation of aluminium, Fe-Al intermetallic creates stable aluminium oxide ( $\alpha$ -Al<sub>2</sub>O<sub>3</sub>) on their surfaces, which contributes positively to corrosion behaviors at high temperatures [8]. The ordered  $\beta$ 2 phase exists within the composition range 36–50 at. % Al at room temperature, according to the FeAl phase diagram [9]. The amount of aluminium in iron aluminides is high enough to form a compact, well-adhered Al<sub>2</sub>O<sub>3</sub> coating on the surface [10].

Some stainless steel storage tanks and pipes were reported to have insufficient corrosion resistance due to molten salts, resulting in molten salt leaks. This problem can be overcome by investigating the corrosion behaviour and mechanism of stainless steel in molten salt. Goods and Bradshaw [11] identified the complex multiphase surface oxide generated on the stainless steel sample in Solar Salt, which consisted primarily of ferrochromium spinel, iron oxide, and sodium ferrite.

This research used computer modelling techniques employing the Ab initio method to investigate the effect of Pt and Ru ternary alloying on physical, mechanical and structural properties of the binary Fe-Al alloy with space group Pm-3m. We have particularly calculated equilibrium cell parameters, elastic constants, moduli and phonon dispersion frequencies. We observed that doping with Pt and Ru yielded better stability, ductility and hardness.

## 2. Methodology

First-principles calculations were performed on the binary Pm-3m-FeAl and ternaries FePtAl<sub>2</sub> and (FeRuAl<sub>2</sub>)<sub>3</sub> to determine their structural, mechanical and dynamical properties. The ternaries FePtAl<sub>2</sub> and (FeRuAl<sub>2</sub>)<sub>3</sub> were harvested from the ground state phase diagram constructed using the Universal Cluster expansion (UNCLE) technique [12]. We employed the density functional theory (DFT) [13] method within the Generalized Gradient Approximation (GGA) [14] using the Vienna Ab initio Simulation Package (VASP) [15]. The Perdew-Berke-Ernzerhof (PBE) functional was applied. A plane-wave cut-off energy of 270 eV and a K-point spacing of 0.5 1/Å was found to be sufficient to successfully converge the internal energies to within 0.001 eV. The elastic constants were calculated using a strain of 0.005. The PHONON code [16] was used to calculate the phonon dispersion curves along high-symmetry lines in the Brillouin zone [17]. An interaction range of 10.0 Å and atomic displacement 0.02 in the +/- direction were applied.

## 3. Results and discussion

### 3.1 Structural properties

Table 1 presents the GGA calculated equilibrium cell parameters for the binary bulk Pm-3m-FeAl and doped ternary P4/mmm-FePtAl<sub>2</sub> and Immm-(FeRuAl<sub>2</sub>)<sub>3</sub> alloys. Available experimental values are also presented. Our calculated cell parameters for the bulk FeAl were predicted to be more than 95 % in good agreement with the experimental data, hence the method employed is valid for these systems.

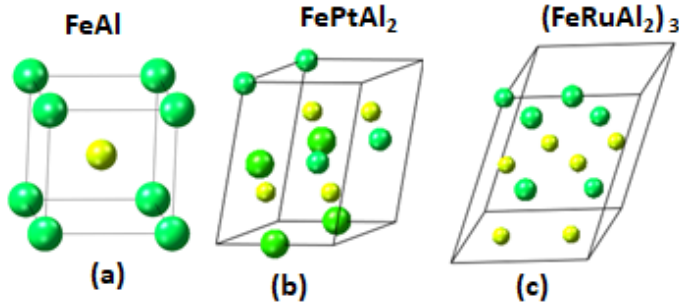


**Fig. 1.** Crystallography of (a) FeAl, (b) FePtAl<sub>2</sub> and (c) (FeRuAl<sub>2</sub>)<sub>3</sub> systems.

**Table 1.** Calculated and experimental equilibrium lattice parameters for Pm-3m-FeAl, P4/mmm-FePtAl<sub>2</sub> and Immm-(FeRuAl<sub>2</sub>)<sub>3</sub> alloys.

Lattice Parameter	Pm-3m-FeAl	P4/mmm-FePtAl <sub>2</sub>	Immm-(FeRuAl <sub>2</sub> ) <sub>3</sub>
a (Å)	2.868	2.982	4.159
Exp. [18]	2.908		
b (Å)	-	-	7.207
c (Å)	-	5.279	5.893
V (Å <sup>3</sup> )	23.539	52.300	152.96

### 3.2 Mechanical Properties

Table 2 present the GGA calculated elastic constants, moduli, and Pugh ratio for the cubic Pm-3m-FeAl, tetragonal P4/mmm-FePtAl<sub>2</sub> and orthorhombic Immm-(FeRuAl<sub>2</sub>)<sub>3</sub> alloys under study. Calculations of elastic constants ( $C_{ij}$ ) are essential in gaining insights into the material's mechanical stability, response to an externally induced stress, and elastic properties which can be derived from ground-state total-energy calculations. The Taylor expansion of the total energy of a strained system [19] was used to calculate the elastic constants.

$$U(V, \varepsilon) = U(V_0, 0) + V_0 \left[ \sum_i \tau_i \varepsilon_i \xi_i + \frac{1}{2} \sum_{ij} C_{ij} \varepsilon_i \varepsilon_j \xi_j \right], \quad (1)$$

where  $U(V_0, 0)$  is the energy of the unstrained system with equilibrium volume  $V_0$ ;  $\tau_i$  and  $\xi_i$  are elements in the stress tensor and a factor taking care of the Voigt index, respectively. Cubic crystal systems contain three ( $c_{11}$ ,  $c_{12}$ ,  $c_{44}$ ) independent and one dependent ( $C'$ ) elastic constants. For the cubic crystals to be considered mechanically stable, the following necessary Born stability criterion must be satisfied [20].

$$C_{11} + 2C_{12} > 0, C_{11} > |C_{12}| \text{ and } C_{44} > 0 \quad (2)$$

Based on these three independent crystal elastic constants, we deduced the macroscopic elastic bulk (B) and shear (G) moduli using the Voigt [21] and Reuss [22] estimates of simple and linear relations between the isotropic bulk and shear moduli of polycrystalline constants. Moreover, Hill showed that the Voigt and Reuss expressions approximate upper and lower bounds, respectively, and proposed an arithmetic average moduli value [23], hence our moduli are reported according to the Hill average. The bulk modulus quantifies the material's resistance to compression under applied pressure, while the shear defines resistance to deformation against external forces.

Tetragonal and orthorhombic crystals, there are six ( $C_{11}, C_{12}, C_{13}, C_{33}, C_{44}, C_{66}$ ) and nine ( $C_{11}, C_{22}, C_{33}, C_{12}, C_{13}, C_{23}, C_{44}, C_{55}, C_{66}$ ) independent elastic constants, respectively. We note that the values of the elastic constants for both the binary and ternary systems satisfy the necessary stability conditions, suggesting mechanical stability. Moreover, the bulk and shear moduli are significantly higher, suggesting good mechanical hardness and deformation resistance. To determine the ductility of our materials, we calculated the Pugh (B/G) [24], the ratio of solids. Pugh proposed that a material is considered ductile if B/G is greater than the critical value of 1.75 and brittle when less than 1.75. From our results, we observed that the B/G ratio of the binary FeAl is less than the required threshold value of  $>1.75$ , implying brittleness. This is in good agreement with the fact that the system suffers limited ductility at temperatures below 873 K; hence the need to introduce Pt and Ru as third metal to enhance ductility. We noticed that the B/G values are greater than 1.75 for the ternaries FePtAl<sub>2</sub> and (FeRuAl<sub>2</sub>)<sub>3</sub> alloys, suggesting ductility. Interestingly, we noted that the ternary alloying significantly increased both the bulk modulus and B/G ratio of the binary FeAl, hence enhancing hardness and ductility.

**Table 2.** Elastic constants and moduli for FeAl, FePtAl<sub>2</sub>, and (FeRuAl<sub>2</sub>)<sub>3</sub> alloys.

Properties (GPa)	Pm-3m-FeAl [18] Cubic	P4/mmm-FePtAl <sub>2</sub> Tetragonal	Immm-(FeRuAl <sub>2</sub> ) <sub>3</sub> Orthorhombic
C <sub>11</sub>	207.07	214.11	332.37
C <sub>12</sub>	90.06	136.47	88.48
C <sub>13</sub>	-	123.60	136.14
C <sub>33</sub>	-	325.38	338.61
C <sub>23</sub>	-	-	124.30
C <sub>22</sub>	-	-	367.09
C <sub>55</sub>	-	-	123.30
C <sub>44</sub>	137.66	111.33	105.27
C <sub>66</sub>	-	120.01	85.01
C' (C <sub>11</sub> - C <sub>12</sub> )/2	58.505	38.820	121.945

B	129.06	168.99	192.88
G	106.00	93.19	108.66
B/G	1.217	1.813	1.775

### 3.3 Vibrational frequency Curve

To determine the dynamical stability of the Pm-3m-FeAl, P4/mmm-FePtAl<sub>2</sub> and Immm-(FeRuAl<sub>2</sub>)<sub>3</sub> alloys, the phonon dispersion frequencies along high symmetry directions in the Brillouin zone were calculated employing a 1x1x1 cell size. Systems are considered dynamically stable if all vibrational frequencies are positive. We observed that both the Binary FeAl structure and the ternary FePtAl<sub>2</sub> and (FeRuAl<sub>2</sub>)<sub>3</sub> alloys (Figure 1) showed no presence of soft modes (negative frequencies) along high symmetry directions, suggesting dynamical stability of the lattice structures. This is in good agreement with the elastic constants' predictions.

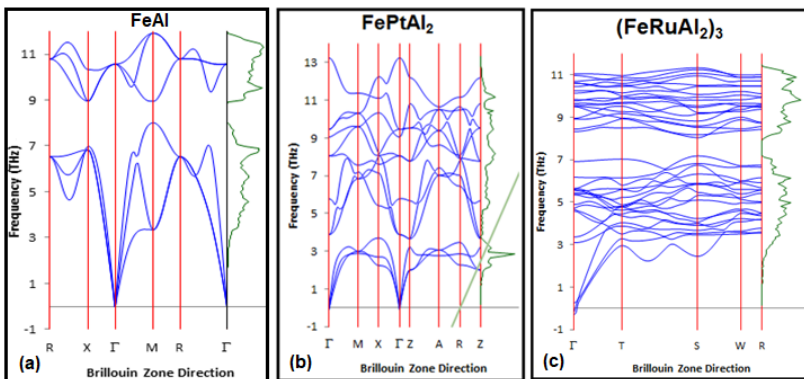


Fig. 2. Phonon dispersion curves of (a) FeAl, (b) FePtAl<sub>2</sub> and (c) (FeRuAl<sub>2</sub>)<sub>3</sub> systems.

### Conclusion

Density functional theory-based first-principles calculations were successfully performed to investigate the effect of Pt and Ru ternary alloying on the mechanical and dynamical properties of the binary Pm-3m-FeAl alloy. The elastic constants showed that both binary FeAl and ternary Fe-Y-Al systems were mechanically stable since all the Born stability criterion were satisfied. This is validated by the phonon dispersion curves which showed only positive vibrational frequencies along high symmetry directions in the Brillouin zone. The bulk moduli were predicted to be higher in Fe-Pt/Ru-Al than in FeAl, suggesting enhancement in mechanical hardness. Moreover, the Pugh is less than 1.75 in FeAl and greater than 1.75 in Fe-Pt/Ru-Al, suggesting a significant enhancement in ductility. The enhancement in mechanical hardness and ductility suggest that the Fe-Pt/Ru-Al systems are promising materials for coating applications.

### Acknowledgments

This work was done at the University of Limpopo at the Materials Modelling Centre (MMC) research unit. The Centre for High-Performance Computing (CHPC) based in Cape Town is acknowledged for its computing resources. The Department of Science and Innovation Initiative is widely acknowledged for its support. The National Research Fund is appreciated for their financial support.

## References

1. X. Li, A. Scherf, M. Heilmaier and F. Stein, *J. Phase Equilib. Diffus.*, **39**, 162-173 (2016).
2. H. Safari and H. Nahvi, *Int. J. Crashworthiness*, **23**, 645-659 (2017).
3. J. P. Flores-de los Rios, E. Haupe-Padilla, M. A. Espnosa-Medina, M. I. Ferrer-Sánchez, R. G. Bautista-Margulis, G. Carbajal-de Torre, L. Bejar-Gómez, J. G. Chacon-Nava and A. Martinez-Villafane, *Int. J. Electrochem. Sci.*, **10**, 2141-2154 (2015).
4. B. M. Mutasa, *Mater. Eng. Sci.* (Blacksburg, Virginia, 1997).
5. R. W. Schutz, *Corrosion*, **59**, 1043 (2003).
6. A. Fones and G. Hatton, *Platinum Metals Rev.*, **58**, 54–57 (2014).
7. C. S. Mkhonto, H. R. Chauke and P. E. Ngoepe, *J. S Afr. Inst. Min. Metall.*, **117**, 1-6 (2017).
8. K. M. Doleker, *J. Mater. Eng. Perfor.*, **29**, 3220 – 3232 (2020).
9. H. I. Sozen, T. Hickel and J. Neugebauer, Max-Planck-institut für eisenforschung GmbH, Mx-Planck-Str. 1, Dusseldorf, Germany., **40237**, 1-11 (2021).
10. J. Cebulski, D. Pasek, M. Bik, K. Świerczek, P. Jeleń, K. Mrocza, J. Dąbrowa, M. Zajusz, J. Wyrwa and M. Sitarz, *Corrosion Sci.*, **164**, 108344(1)-108344(14) (2020).
11. S. H. Goods, R. W. Bradshaw, *J. Mater. Eng. Perfor.*, **13**, 78-87 (2004).  
R. V. Mises and Z. Agnew, *Math. Mech.*, **8**, 161-185 (1928).
12. D. Lerch, O. Wieckhorst, G. L. W. Hart, R. W. Forcade and S. Muller, *Simul. Mater. Sci. Eng.*, **17**, 1-9 (2009).
13. A.E. Mattson, P.A. Schultz, M.P. Desjarlais, T.R. Mattsson and K. Leung, *Mod. Simul. Mater. Sci. and Eng.*, **13**, 1-32 (2005).
14. J.P. Perdew, K. Burke and M. Ernzerhof, *Phys. Rev. Lett.*, **77**, 3865-4065 (1996).
15. G. Kresse, M. Marsman, and J. Furthmüller, VASP the guide (*Comp. Mater. Phys., Faculty of Physics, Universität Wien*, 2018).
16. R. M. Martin and K. Kunc, *Phys. Rev. Lett.*, **48**, 406-440 (1982).

17. H. J. Monkhorst and J. D. Pack, *Phys. Rev. B*, **13**, 5188-5190 (1976).
18. M. Zamanzade, A. Barnoush and C. Motz, *Crystals*, **6**, 1-29 (2016).
19. L. Fast, J. M. Wills, B. Johansson and O. Eriksson, *Phys. Rev. B*, **51**, 17431 (1995).
20. B. B. Karki, G. J. Ackland and J. Crain, *J. Phys.: Condens. Matter*, **9** (1997).
21. W. Voigt, *Lehrbuch der Kristallphysik* (Leipzig, Taubner, 1928).
22. A. Reuss, *Z. Angew. Math. Mech*, **9**, 49-58 (1929).
23. R. Hill, *Proc. Soc. London A*, **65**, 350-360 (1952).
24. S. F. Pugh, *Philos. Mag.*, **45**, 823-850 (1954).
25. M. Zamanzade, A. Barnoush and C. Motz, *Crystals*, **6**, 1-29 (2016).